Multidiszciplináris tudományok, 13. kötet, 2. sz. (2023), pp. 78–86 **https://doi.org/10.35925/j.multi.2023.2.7**

INVESTIGATIONS ON THE LIMIT-POINT BUCKLING OF CURVED BEAMS

Abderrazek Messaoudi
PhD student, Institute of Applied Mechanics, University of Miskolc
3515 Miskolc-Egyetemváros, e-mail: abderrazek.messaoudi@uni-miskolc.hu

László Péter Kiss
associate professor, Institute of Applied Mechanics, University of Miskolc
3515 Miskolc-Egyetemváros, e-mail: mechkiss@uni-miskolc.hu

Abstract

Calculating the critical load that could lead to beam failure through buckling is a complex issue. This paper intends to analyze the stability of arches taking into account how the curvature, material properties, load positions and geometry affect the behavior. Unlike in many other articles, the impact of the bending moment on the membrane strain is also incorporated into the model. To derive the buckling equilibrium equation, the principle of virtual work is applied, and analytical solutions for the limit point buckling are provided. It is worth noting that the load location has a significant impact on the buckling load, and this relationship is strongly associated with the ratio of the arch length to the radius of the gyration of the structure. It is found that in the case of fixed arches, two stable equilibrium branches and one unstable branch can be observed when buckling is possible. When the load is positioned sufficiently far from the crown point, the load-carrying capacity of the structure improves.

Keywords: *arch, radial load, buckling, limit point, nonlinear*

1. Introduction

Arches are common architectural features that are used commonly. They are employed to support a roof, bridge, or to span an opening. When arches are subjected to a compressive load, they may become unstable and experience a phenomenon known as buckling. Therefore, it is essential to consider the potential of the limit point buckling in arch design to ensure structural stability and safety (Timoshenko et al., 1961). In essence, the failure mode of buckling in arches refers to the arch collapsing inward along the plane of curvature. The issue of buckling has been the subject of extensive research and analysis in the past and present, and there exists a considerable body of work on this topic (Simitses, 1976), (Bradford et al., 2015), (Simitses et al., 2006). It is essential to understand the factors that contribute to buckling of arches, such as the material properties, and the geometrical features. By identifying these factors and incorporating them into the design process, engineers can create arches that are better equipped to resist buckling issue and ensure the safety and stability of the structure. Several studies have investigated the impact of a concentrated force at the crown point of arches (Bradford et al., 2015), (Gjelsvik et al., 1962), (Pi et al., 2008), (Pi et al., 2017). Researchers have also used a radial concentrated load in the vicinity of the crown as a substitute for a precisely located concentrated load. This approach is more practical to implement in experimental settings. By using radial concentrated loads in experiments, researchers can gain a better understanding of the behavior of arches under different

loading conditions to improve the design of arches in order to resist buckling and collapse. Some numerical studies, such as those conducted by (Yang et al., 1995), (Kuo et al., 1990), have discovered that the position of the radial load can have an impact on both nonlinear equilibrium and limit buckling load. The effect of an arbitrary load for fixed supports is addressed in (Kiss, 2020), however, the article fails to deliver an in-depth analysis about the topic.

Overall, it can be concluded that the available literature lacks sufficient analysis regarding the nonlinear equilibrium and buckling of arches under asymmetrical loading conditions, including radial concentrated forces. Additionally, gaining knowledge about how load position affects the buckling load of fixed arches could prove to be highly beneficial in engineering applications. The present study focuses on examining the stability of fixed arches that have an *I*-shaped cross-section and are subjected to radial concentrated load. To derive the governing pre-buckling equilibrium equation, the principle of virtual work is employed, and special attention is paid to accounting for the effect of the bending moment on the membrane strain.

2. Mechanical model

We shall consider a fixed-fixed arch as it is shown in *Figure 1*. The cross-sectional coordinates are η, ζ and the axis ξ coincides with the circumferential direction. Axis η is a major principal axis of the arch. The length of the arch is *S*, the included angle is *2θ*, the initial constant radius of curvature is *R*. Furthermore, φ and *s* are the angle and arc coordinates. The load is applied at a coordinate *α = [0; θ]*. If α = 0, it is a limit case with the load being at the symmetry axis of the arch. It is assumed that the behavior of the material is linearly elastic and isotropic.

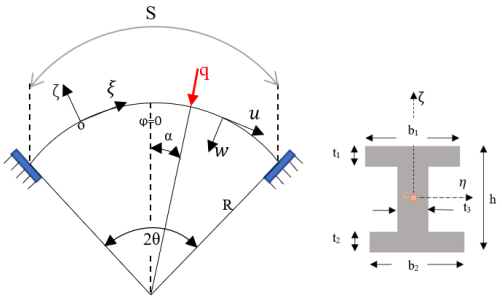

Figure 1. *Arch geometry*

The membrane strain at an arbitrary point on the centroidal axis (ζ = 0) is given by (Szeidl et al., 2015):

$$\varepsilon_m = \frac{\mathrm{d}u}{\mathrm{d}s} + \frac{w}{R} + \frac{1}{2}\left(\frac{u}{R} - \frac{\mathrm{d}w}{\mathrm{d}s}\right)^2 \tag{1}$$

where *u* and *w* are the axial and radial displacements on the centroidal axis, respectively. The nonlinear term *0.5(dw/ds)*^{2} accounts for the large rotations. The axial force *N* and the bending moment *M* can be represented as follows (Szeidl et al., 2015) using the Hooke law:

$$N = A\varepsilon_m - \frac{I_e}{R}\left(\frac{1}{R}\frac{\mathrm{d}u}{\mathrm{d}s} - \frac{\mathrm{d}^2w}{\mathrm{d}s^2}\right), \quad M = -I_e\left(\frac{\mathrm{d}^2w}{\mathrm{d}s^2} + \frac{w}{R^2}\right), \quad N + \frac{M}{R} = A_e\varepsilon_m \tag{2}$$

with I_e being the moment of inertia about the major principal axis η and A_e being the E- weighted area of the cross-section:

$$(I_e) = E \int_A (\zeta^2)\, \mathrm{d}A \tag{3}$$

Using the virtual work principle, the pre-buckling equilibrium configuration can be established (Szeidl et al., 2015). For mathematical simplification we shall introduce $W = w/R$ and $U = u/R$ are dimensionless displacements. Fundamental equations (1)–(3) yield (Kiss, 2020) equilibrium equations

$$\varepsilon_m^{'} = 0, \qquad W^{''''} + \left(\mu^2 + 1\right) W^{''} + \mu^2 W = \mu^2 - 1, \tag{4}$$

with *d(...)/ds=(...)'* and

$$\mu^2 = 1 - \kappa\varepsilon_m; \qquad \kappa = \frac{A_e R^2}{I_e} = \frac{R^2}{r^2}; \qquad \lambda = \sqrt{\kappa}\theta^2 = \frac{S\theta}{2r}. \tag{5}$$

In which λ is the slenderness of the arch (Bradford et al., 2002) and r is the radius of gyration of the cross-section about its major principal axis η.

The displacement and rotation are zero at the supports, whereas all fields are continuous, with the exception of the dimensionless shear force distribution, which displays a discontinuity of value Q at α:

$$\begin{gathered} W|_{\varphi=-\theta} = W^{''}\Big|_{\varphi=-\theta} = W|_{\varphi=\theta} = W^{''}\Big|_{\varphi=\theta} = 0, \\ W|_{\varphi=-\alpha} = W|_{\varphi=+\alpha} \qquad W^{'}\Big|_{\varphi=-\alpha} = W'|_{\varphi=+\alpha}, \\ W^{''}\Big|_{\varphi=-\alpha} = W^{''}\Big|_{\varphi=+\alpha} \qquad - W^{'''}\Big|_{\varphi=-\alpha} + W^{'''}\Big|_{\varphi=+\alpha} = -\frac{2Q}{\theta} \end{gathered} \tag{6}$$

where Q is the dimensionless load defined by *Q=qR^2θ/2I_e*. Thus, the membrane strain is constant and equal to its average as per Equation $(4)_1$. Using the solution to Equation $(4)_2$ and the constant membrane strain finding, it yields a nonlinear equilibrium equation which relates the dimensionless strain parameter μ and the dimensionless load Q as

$$\int_{-\theta}^{\theta} \varepsilon_m(\varphi)\mathrm{d}\varphi \simeq \int_{-\theta}^{\theta} \left[U^{'} + W + \frac{1}{2}\left(W^{'}\right)^2\right] \mathrm{d}\varphi - 2\theta\varepsilon_m = B_1 + B_2 Q + B_3 Q^2. \tag{7}$$

Due to the shallowness, the impact of the axial displacement on the rotation can be disregarded (Pi et al., 2017). Based on the information provided above, closed-form calculations can be set up for the constants B_1, B_2 and B_3, which are functions of α, θ, λ, μ. For more details, we advise the reader to refer to (Kiss, 2020).

3. Results and Discussion

In this section, we present some illustrative results to investigate the effect of load position and geometric properties on the stability of the fixed-fixed arch. The purpose of this study is to extend (Kiss, 2020) and gain detailed insights into the behavior of these structures when they are subjected to an arbitrary radial concentrated force. To simplify the analysis, it is assumed that the material used in the

construction of the arch is homogeneous. This means that the modulus of elasticity *(E)* and the Poisson ratio (ν) of the material remain constant throughout the entire arch. The values for these constants have been taken as $E = 2.1e5$ N/mm^2 and $\nu = 0.3$. *Figure 1* provides a detailed representation of the geometrical data for the *I*-cross section. The section depth is denoted as *h* and has a value of *256* mm. The flange width is denoted as $b_1=b_2$ and has a value of *146* mm. The flange thickness is denoted as $t_1 = t_2$ and has a value of *10.9* mm. The web thickness is denoted as t_3 and has a value of *6* mm. The quotient of the arch length *S* and the radius of gyration $r = (I/A)^{0.5}$ is selected to have seven values: *50, 75, 100, 150, 200, 250* and *300*.

In *Figure 2*, the dimensionless buckling loads are plotted against the semi-vertex angle for the selected *S/r* ratios with the assumption that the load is applied at the crown point ($\alpha = 0$). It is discovered that the critical load increases as the *S/r* quotient increases and that the arches with a higher *S/r* ratio can carry greater loads.

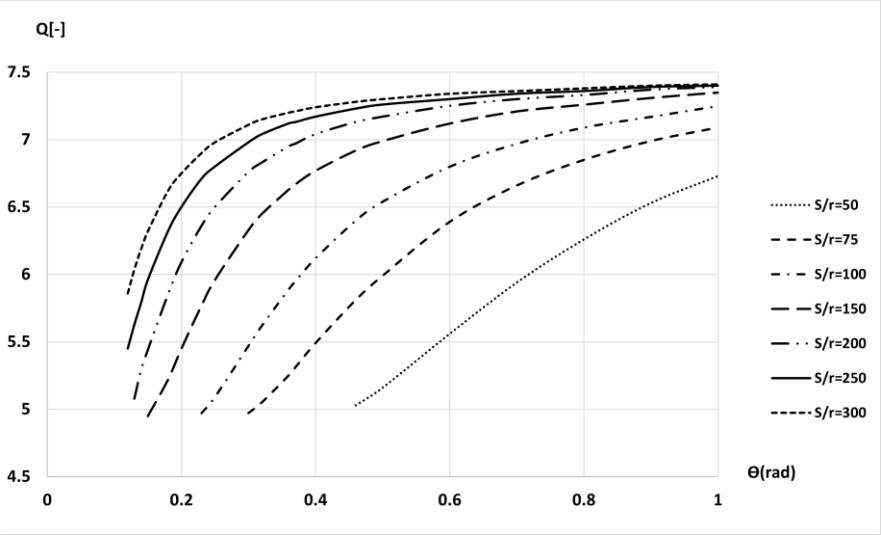

Figure 2. *Critical loads of a fixed arch for different values of S/r*

This increase in the radius of curvature leads to a reduction in the bending moment within the arch, resulting in a higher load-carrying capacity. It is observed that when the semi-vertex angle $0.85 < \theta$ and $200 < S/r$, the solutions of the critical load tend to be less independent of these parameters, which in turn leads to little or no difference in the critical load. It can be seen that when the load is applied vertically at the crown point, the curves shift to the left when *S/r* is increased, i.e., buckling may occur for smaller included angles.

The impact of load position denoted by α/θ on the dimensionless buckling loads of the analyzed arch having $S/r = 150$ is presented in *Figure 3*. The results indicate that the effect of load location is considerably dependent on the semi-vertex angle θ. In the case of arches having $\theta = 0.2$, the buckling load increases monotonically with α/θ. However, for arches with $\theta = 0.4$ and $\theta = 1$, the buckling load initially experiences a slight decline until $\alpha/\theta = 0.15$ and then increases. Meanwhile, the buckling load of the arches having $\theta = 0.6$ and $\theta = 0.8$ first decreases until $\alpha/\theta = 0.16$ and then increases.

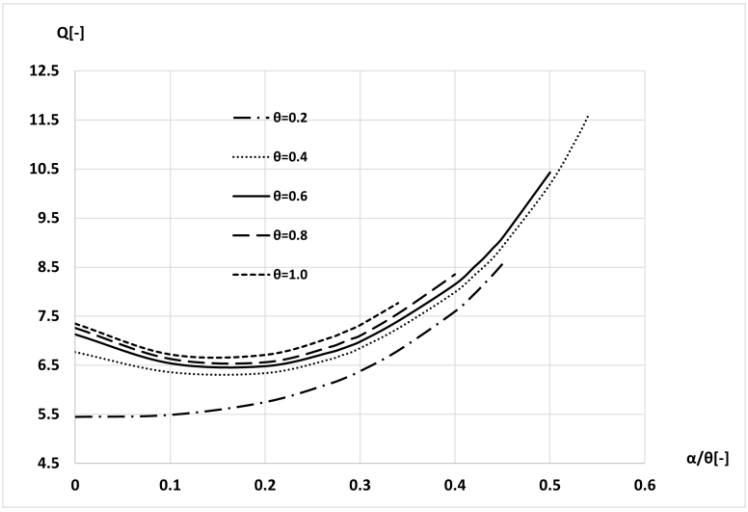

Figure 3. *Effect of load position α/θ on the buckling load of arches having S/r = 150*

In the case of arches with *S/r = 150*, it is investigated how the load position α can affect their behavior as is shown in *Figure 4*. Since one branch always starts from the origin ($Q = 0, \mu = 1$), i.e., $\varepsilon_m = 0$. It is worth noting that the position of the load has a significant impact on determining the curve endpoints, which have different values on the vertical axis. This latter one is greater in terms of the dimensionless load if α is greater. It can be seen also that the intersection point for all curves has the same coordinate at μ = 10.54. The loop always becomes smaller with μ parameter when α increases. As a result, the load-bearing capabilities of arches become even better when the load is placed elsewhere sufficiently far from the crown point. When the load position is changed from the crown position, the critical load decreases due to a small perturbation in the load position ($\alpha = 0.1\theta$) but after that, there is an increase.

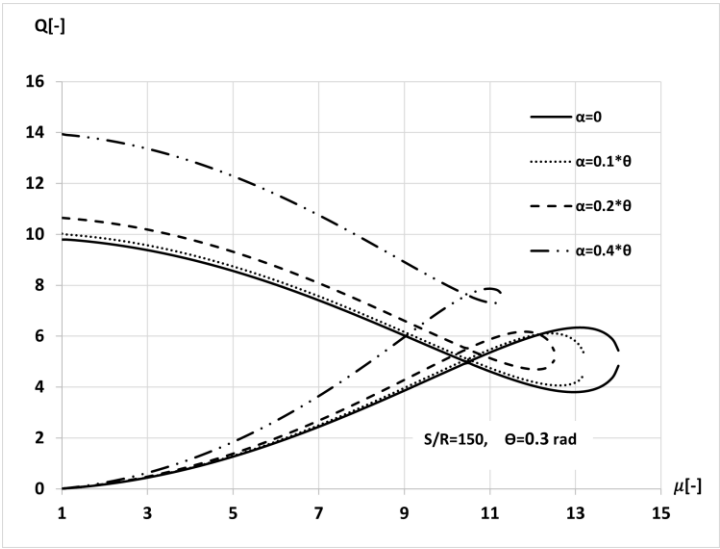

Figure 4. *Dimensionless load in terms of a dimensionless strain parameter μ*

It is found that fixed-fixed arches are not sensitive to small imperfections in load position, unlike pinned-pinned members (Kiss, 2019), i.e., the difference in buckling load of these is small due to a small perturbation in the load position around the crown point.

The nonlinear behavior of an arch, when subjected to a given load position α/θ, is strongly influenced by its modified slenderness. The changes in the dimensionless crown point displacement $W_c = W(\varphi = 0)$ as a function of the dimensionless radial concentrated load Q when the load position has a value of $\alpha/\theta = 0.2$ are illustrated in *Figure 5*. It is revealed that when the modified slenderness λ is greater than *12.6*, the arch exhibits distinct upper and lower limit points. However, at λ = 12.6, these limit points merge into a point of inflection.

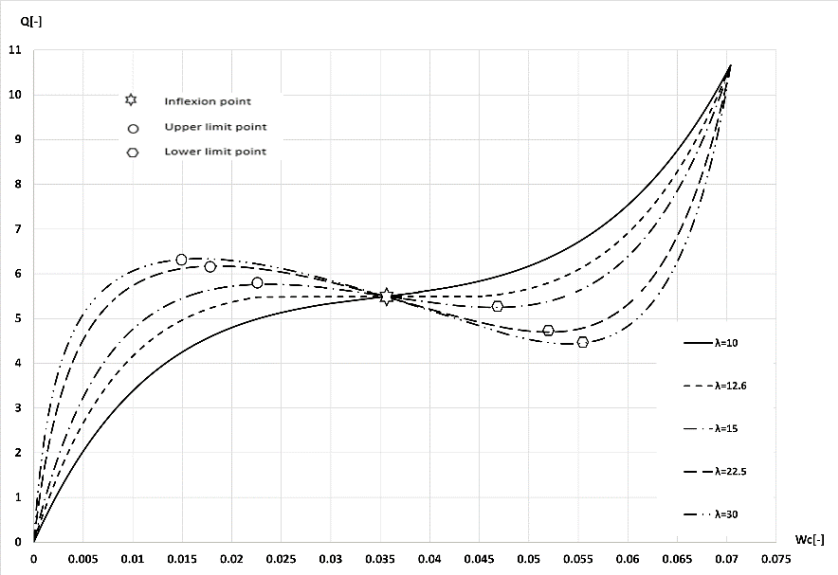

Figure 5. *Arch with $\theta = 0.3$ and $\alpha/\theta = 0.2$: dimensionless load against dimensionless crown point displacement*

For values of λ below *12.6*, the arch does not display any typical buckling behavior. When there is no buckling, there is only one stable branch (see the continuous curve). On the other hand, the number of equilibrium branches increases with λ and it seems to be always three branches (two stable branches and one unstable) unlike the nonlinear behavior of pinned-pinned (Kiss, 2019) arches, where more than three branches can be found generally.

Figures 6 and *7* illustrate the impact of load position on the dimensionless radial displacements *W* and inner forces *(M/NR)* along the length of the arch. The analysis considers a value of $\lambda = 22.5$, and a concentrated load is applied radially at various positions on the right half of the arch. The magnitude of the load corresponds to the upper limit of the same arch when the load is applied at the crown point (given by a dimensionless load $Q = 6.33$). With *N* being the second mode of the flexural buckling load of the fixed -fixed column in axial uniform compression and it has the following formula $I_e\pi^2/0.25S^2$.

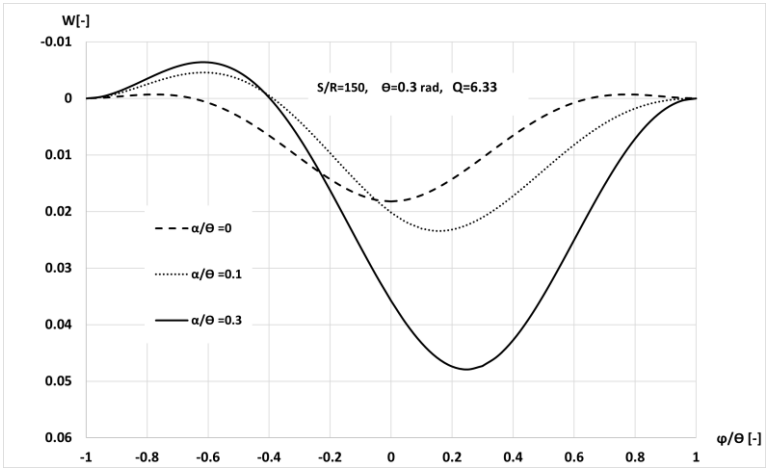

Figure 6. *Effects of the load positions on the dimensionless radial displacement*

It is obvious that the displacement at the load position has the maximum value because it directly experiences the applied load, leading to the most significant deformation within the arch structure. The difference in displacements and bending moments of the arch become greater as the load shifts away from the crown point. It turned out that the bending moment at the right end changes from positive to negative.

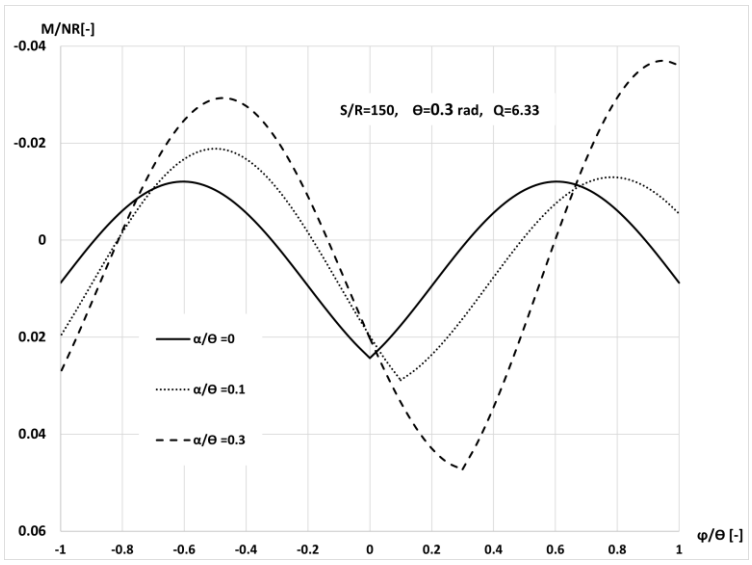

Figure 7. *Effects of the load positions on the dimensionless inner forces*

4. Conclusions

This article focuses on the stability behavior of the fixed-fixed arches with the *I*-cross-section, which are subjected to a radial concentrated load. A one-dimensional beam model based on the Euler-Bernoulli hypothesis was used and the related static pre-buckling equilibrium equations were derived from the

principle of virtual work. It was found that the arch length/radius of gyration ratio *S/r* influenced the buckling load significantly, and the influence was much related to the included angle of the arch. Increasing the value *S/r* leads to an increase in the critical loads. It also turned out that when the load is placed far from the crown point, the buckling load experiences a decrease for a short while and after it increases. As a results, when the load is positioned close to the supports, the structure's ability to bear the load improves, and the buckling load can increase or the arch may not experience buckling. Additionally, it was shown that when *S/r* is smaller than a specific value, the arch does not buckle. There are only three equilibrium branches for the fixed- fixed arches (two stable and an unstable between them) when the buckling can occur.

References

[1] Timoshenko, S. P. and Gere, J. M. (1961). Theory of Elastic Stability. 2nd edn. Engineering Societies Monograps.
[2] Simitses, G. J. (1976). An Introduction to the Elastic Stability of Structures. Prentice-Hall. **https://doi.org/10.1115/1.3423874**
[3] Bradford M. A., Uy, B., Pi, Y.-L. (2006) In-plane elastic stability of arches under a central concentrated load. Journal of Engineering Mechanics, 128 (7), 710-719. **https://doi.org/10.1061/(ASCE)0733-9399(2002)128:7(710)**
[4] Simitses, G. J., Hodges, D. H. (2006). Fundamentals of Structural Stability. Butterworth-Heinemann.
[5] Gjelsvik, A. and Bodner, S. R. (1962). Energy criterion and snap-through buckling of arches. Journal of Engineering Mechanics ASCE, 88 (5), 87-134. **https://doi.org/10.1061/JMCEA3.0000327**
[6] Pi, Y. L., Bradford, M. A., Tin-Loi, F. (2008). Non-linear in-plane buckling of rotationally restrained shallow arches under a central concentrated load. International Journal of Non-Linear Mechanics, 43 (1), 1-17. **https://doi.org/10.1016/j.ijnonlinmec.2007.03.013**
[7] Pi, Y.-L., Bradford, M. A., Liu, A. (2017). Nonlinear equilibrium and buckling of fixed shallow arches subjected to an arbitrary radial concentrated load. International Journal of Structural Stability and Dynamics, 17 (8), 1-17. **https://doi.org/10.1142/S0219455417500821**
[8] Yang, Y. B., Shieh, M. A. (1995). Solution method for nonlinear problems with multiple critical points. AIAA Journal, 28 (12), 2110-2116. **https://doi.org/10.2514/3.10529**
[9] Kuo, S. R., Yang, Y. B. (1995). Tracing postbuckling paths of structures containing multi loops. International Journal of Numerical Methods in Engineering, 38 (23), 4053-4075. **https://doi.org/10.1002/nme.1620382309**
[10] Kiss, L., Szeidl, G. (2015). Nonlinear in-plane stability of heterogeneous curved beams under a concentrated radial load at the crown point. Technische Mechanik, 35 (1), 1-30.
[11] Pi, Y-L., Bradford, M. A. (2012). Non-linear in-plane analysis and buckling of pinned-fixed shallow arches subjected to a central concentrated load. Non-Linear Mechanics, 47 (4), 118-131. **https://doi.org/10.1016/j.ijnonlinmec.2012.04.006**
[12] Kiss, L. P. (2020). Nonlinear stability analysis of FGM shallow arches under an arbitrary concentrated radial force. Mechanics and Materials in Design, 16 (1), 91-108. **https://doi.org/10.1007/s10999-019-09460-2**
[13] Bradford, M. A., Uy, B., Pi, Y.-L. (2002). In-plane stability of arches. International Journal of Solids and Structures, 39 (1), 105-125. **https://doi.org/10.1016/S0020-7683(01)00209-8**

[14] Kiss, L. P. (2019). Sensitivity of FGM shallow arches to loading imperfection when loaded by a concentrated radial force around the crown. International Journal of Non-Linear Mechanics, 116, 62. **https://doi.org/10.1016/j.ijnonlinmec.2019.05.009**

[15] Bradford, M. A., Uy, B., Pi, Y.-L. (2002) In -Plane Elastic Stability of Arches under a Central Concentrated Load. Journal of Engineering Mechanics, 128 (7), 710. **https://doi.org/10.1061/(ASCE)0733-9399(2002)128:7(710)**

[16] Kiss, L. P. (2020) Stability of fixed-fixed shallow arches under arbitrary radialand vertical forces. Magazine of Civil Engineering, 95 (3), 31-41.